Hindawi Publishing Corporation
Mathematical Problems in Engineering
Volume 2012, Article ID 534189, 17 pages
doi:10.1155/2012/534189

*Research Article*

# The Nonlinear Behavior of Vibrational Conveyers with Single-Mass Crank-and-Rod Exciters

**G. Füsun Alışverişçi**

*Department of Mechanical Engineering, Yıldız Technical University, 34349 İstanbul, Turkey*

Correspondence should be addressed to G. Füsun Alışverişçi, afusun@yildiz.edu.tr

Received 22 May 2012; Accepted 13 August 2012

Academic Editor: Xing-Gang Yan



The single-mass, crank-and-rod exciters vibrational conveyers have a trough supported on elastic stands which are rigidly fastened to the trough and a supporting frame. The trough is oscillated by a common crank drive. This vibration causes the load to move forward and upward. The moving loads jump periodically and move forward with relatively small vibration. The movement is strictly related to vibrational parameters. This is applicable in laboratory conditions in the industry which accommodate a few grams of loads, up to those that accommodate tons of loading capacity. In this study I explore the transitional behavior across resonance, during the starting of a single degree of freedom vibratory system excited by crank-and-rod. A loaded vibratory conveyor is more safe to start than an empty one. Vibrational conveyers with cubic nonlinear spring and ideal vibration exciter have been analyzed analytically for primary and secondary resonance by the Method of Multiple Scales, and numerically. The approximate analytical results obtained in this study have been compared with the numerical results and have been found to be well matched.

## 1. Introduction

In this work, the vibrating system consists of a cubic nonlinear spring and sinusoidal excitation (ideal source) is studied. It is an ideal system, if there is no coupling between motion of the rotor and vibrating system. In this case, the excitation is completely independent of the system response. Vibrating systems with ideal and nonideal excitations were investigated by number of authors. Kononenko [1] presented the first detailed study on the nonideal problem of passage through resonance. Some numerical studies on dynamic characteristics of a vertical pendulum whose base is actuated horizontally through a slider crank mechanism, where the crank is driven through a DC motor, were performed in [2, 3], and investigations on the properties of the transient response of this nonlinear and nonideal problem showed that near the fundamental resonance region, near a secondary resonance

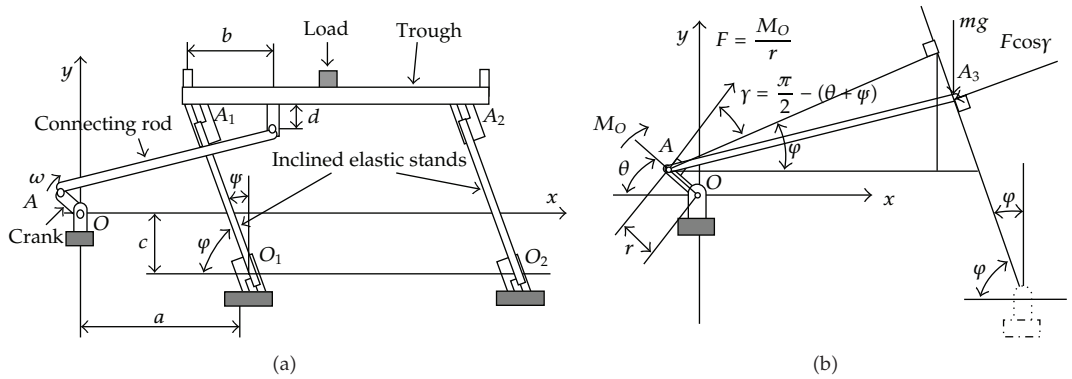


**Figure 1:** (a) Single-mass, crank-and-rod-driven vibrational conveyer, (b) the coercive force applied on the trough.

region, respectively. An overview of the main properties of nonideal vibrating systems was presented by Balthazar et al. [4, 5]. These authors analyzed that the physical model of the ideal vibrating system consists of linear spring and sinusoidal excitation (ideal source) [6], the physical model of the vibrating system consists of linear spring and nonideal source [7], and the physical model of the vibrating system consists of a cubic nonlinear spring and nonideal source [8].

In this study, vibrational conveyers are constituted by a trough and elastic stands of equal length connected to trough inclinedly. Forced vibration motion driven by the crank-and-rod mechanism is given to this system (Figure 1). Crank-and-rod mechanism with elastic connecting rod can also be used and an elastic component added to the operation mechanism slowly increases the amplitude of the system from a low value to the maximum operation amplitude; it functions as elastic component at the initial motion of the conveyer and as rigid component at the continuous operation state. During the vibration motion, the forward and upward motions of the load on the trough are provided. After each contact to the trough, the velocity of forward movement of the load increases. The velocity of forward movement of the load increases until it reaches the maximum velocity of trough. After reaching the maximum velocity, it continues its motion at this velocity [9, 10].

The vibrational conveyers have been analyzed numerically and analytically by the Method of Multiple Scales, for the primary and subharmonic and superharmonic resonance. The stability is analyzed by using an approximate analytical solution. The frequency-response curves show the behavior of the oscillator for the variation of the control parameters. Numerical simulations are performed and the simulation results are visualized by means of the phase portrait, Poincaré map, and Phase portrait.

## 2. The Governing Equations of the Motion

The equations of motion for the vibrating model of system may be obtained by using Lagrange's Equation, *the conveyor empty*:

$$\frac{d}{dt}\left(\frac{\partial T}{\partial \dot{q}_i}\right) + \frac{\partial D}{\partial \dot{q}_i} - \frac{\partial T}{\partial q_i} + \frac{\partial V}{\partial q_i} = Q_i, \tag{2.1}$$

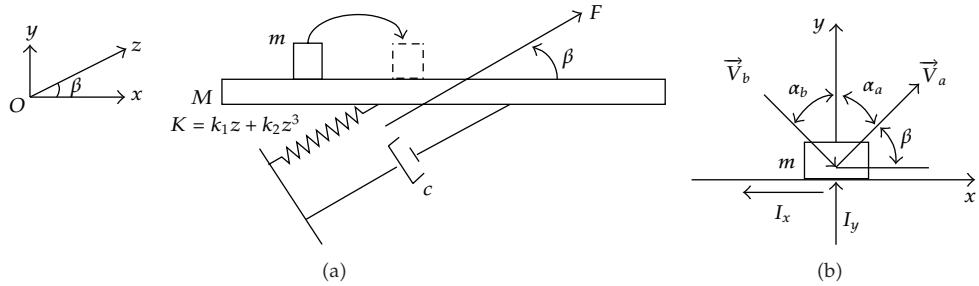


**Figure 2:** (a) Vibrating model of system, (b) material motion.

where $M$ is mass of the trough of the conveyor, $T$ is the kinetic energy

$$T = \left(\frac{1}{2}M\dot{z}^2\right), \tag{2.2}$$

$V$, the potential energy, is

$$V = \frac{1}{2}k_1z^2 + \frac{1}{4}k_2z^4, \tag{2.3}$$

$D$, the Rayleigh Dissipation Function, is

$$D = \frac{1}{2}c\dot{z}^2, \tag{2.4}$$

and $q_i$ is the generalized coordinate. Applying Lagrange's Equation for the coordinate $q_i = z$ gives the differential equations of motion.

Here the measurement values are taken from the position where the components in the same directions of the vertical force applied by the leaf spring on itself and the weight force balances each other. If the mass of the leafs works as spring as well as the mass of the $AA_3$ connecting rod, the changes in the angle $\psi$ and moment $M_0$ applied on the crank arm by the motor are neglected, and the coercive force in the vibration motion can be written as below (Figure 2(b)) [11, 12], then the coercive force becomes

$$\begin{gathered} F(t) = F\cos\gamma, \qquad \gamma = \left(\frac{\pi}{2}\right) - (\theta + \psi), \qquad \cos\gamma = \sin(\theta + \psi), \qquad \Theta = \theta - \psi, \qquad \Theta = \omega t, \\ F(t) = \left(\frac{M_O}{r}\right)\sin\omega t, \qquad F = m_t r\omega_n^2 = m_t r\frac{k_1}{m_t} = rk_1, \end{gathered} \tag{2.5}$$

where $m_t$ is the total vibrating mass, $r$ is the length of the crank, then one can write the generalized force $Q_1$

$$\begin{gathered} M\ddot{z} + c\dot{z} + k_1z + k_2z^3 = F(t), \\ \ddot{z} + \frac{c}{M}\dot{z} + \frac{k_1}{M}z + \frac{k_2}{M}z^3 = \frac{1}{M}F(t). \end{gathered} \tag{2.6}$$

Rewriting (2.6) in terms of variables, it will obtained, where $c$ is damping coefficient, $k_1$ is the linear spring coefficient, and $k_2$ is the cubic spring coefficient, that $\omega_n$ is the natural frequency: $\omega_n^2 = k_1/M$, $\varepsilon = 1/M$,

$$\ddot{z} + \omega_n^2 z = \frac{1}{M}\left(F(t) - c\dot{z} - k_2 z^3\right), \tag{2.7}$$

where $b = c/2M$, $\alpha = k_2/M$,

$$\ddot{z} + \omega_n^2 z = \frac{F}{M}\sin(\theta + \varphi) - 2b\dot{z} - \alpha z^3. \tag{2.8}$$

The conveyor was filled with material, during one of the motions of the trough, and the load may be in a ride, slide, or flight phase, depending on the actual accelerations, velocities, and displacements of the load and trough. These various phases of motion are analyzed.

(i) *Flight Phase* (when $y_t'' < -g$). A flight phase occurs if the normal force becomes zero. At the start of a flight the load and trough have the same $y$-coordinate and $y'$-velocity. The load loses contact with the trough and is said to travel in a "*flight phase.*" The governing equations of motion then are as follows: for the trough: (2.8) (conveyor empty); for the material is moving under the action of gravity which,

$$x_m'' = 0, \qquad y_m'' = -g. \tag{2.9}$$

The end of flight phase can be derived from the condition of equal $y$ coordinates and terminates in an "*impact*" with the trough

$$y_m = y_t. \tag{2.10}$$

This oblique impact is considered to be instantaneous and "*perfectly plastic*" in the $y$ direction. Considering the principle of conservation of the total momentum and the Newton's Law of Impact,

$$x_t' = y_t' \cot\beta. \tag{2.11}$$

"*friction impact*", in the $x$ direction, "$t$" and "$m$" represent the parameters of the trough and the material particle, respectively. "$a$" and "$b$" represent the parameters "after" and "before" the impact, respectively (Figure 2(b)):

$$\begin{gathered} I_x = -\mu I_y \\ y_a' = -e y_b', \qquad v_a \cos\alpha_a = e v_b \cos\alpha_b. \end{gathered} \tag{2.12}$$

The change of the velocity of the load during an impact with the trough is related to the total linear impulse at time of flight phase, by the linear momentum equation

$$\begin{gathered} m\vec{V}_a - m\vec{V}_b = I \\ I_x = m(v_a \sin\alpha_a - v_b \sin\alpha_b), \qquad I_y = m(v_a \cos\alpha_a + v_b \cos\alpha_b) \\ m\left(\underbrace{v_a \sin\alpha_a}_{\dot{x}_a} - \underbrace{v_b \sin\alpha_b}_{\dot{x}_b}\right) = -\mu m\left(\underbrace{v_a \cos\alpha_a}_{\dot{y}_a} + \underbrace{v_b \sin\alpha_b}_{-\dot{y}_b}\right) \\ (\dot{x}_{m_a} - \dot{x}_{m_b}) = \pm\mu(\dot{y}_{m_a} - \dot{y}_{m_b}). \end{gathered} \tag{2.13}$$

The coefficient of friction times the change in velocity of the load along the $y$ direction due to impact

$$(\dot{x}_{m_a} - \dot{x}_{m_b}) = \operatorname{sign}\mu(\dot{y}_{m_a} - \dot{y}_{m_b}), \tag{2.14}$$

where the negative or positive signs for the frictional force $f$ sign are +1.0 or −1.0 as $(\dot{x}_{m_b} - \dot{x}_{t_b}) < 0$ or $> 0$. If the flight ends with a tangential velocity of the load that is not equal to that of the trough, a positive or negative slide phase occurs, depending on the sign of this difference, until the velocities become equal.

(ii) *Ride Phase*. In this case the trough and the load are as one body. If the load's velocity and trough's velocity are equal:

$$\dot{y}_m = \dot{y}_t, \qquad y_m = y_t, \tag{2.15}$$

the conditions are such that

$$\begin{gathered} |\ddot{x}_t| \le \mu(\ddot{y}_t + g), \\ \dot{x}_m = \dot{x}_t. \end{gathered} \tag{2.16}$$

For the trough, where $m$ is mass of the conveyed material on the trough of the conveyor, $T$ is the kinetic energy

$$T = \left(\frac{1}{2}M\dot{z}^2\right) + \left(\frac{1}{2}m\dot{z}^2\right), \tag{2.17}$$

$V$, the potential energy, is

$$V = \frac{1}{2}k_1 z^2 + \frac{1}{4}k_2 z^4 + mg\sin\beta z, \tag{2.18}$$

$D$, the Rayleigh Dissipation Function, is

$$D = \frac{1}{2}c\dot{z}^2 \tag{2.19}$$

$$\begin{gathered} (M+m)\ddot{z} + c\dot{z} + k_1 z + k_2 z^3 = F(t) - mg\sin\beta \\ \ddot{z} + \frac{c}{M+m}\dot{z} + \frac{k_1}{M+m}z + \frac{k_2}{M+m}z^3 = \frac{1}{M+m}F(t) - \frac{mg}{M+m}\sin\beta \end{gathered} \tag{2.20}$$

rewriting (2.20) in terms of variables, $m$ is mass of the conveyed material on the trough of the conveyor, $g$ is acceleration due to gravity, $\omega_n^2 = k_1/(m+M)$, $2b = c$, $\varepsilon = mg/(M+m)$, $\alpha = k_2$, $G = mg/M + m$,

$$\ddot{z} + \omega_n^2 z = \varepsilon\left[F\sin(\theta+\varphi) - 2b\dot{z} - \alpha z^3\right] - G\sin\beta \tag{2.21}$$

And, for the material,

$$x_m = x_t, \qquad \dot{x}_m = \dot{x}_t. \tag{2.22}$$

(iii) *Slide Phase.* Sliding may start when the accelerations of the load and the trough are equal. Vertical component of trough's acceleration is greater than acceleration of gravity

$$\left[\ddot{y}_t > -g\right], \qquad \left[\left\{|\ddot{x}| > \mu(g+\ddot{y}_t)\right\} \text{ or } \left\{\dot{x}_m \neq \dot{x}_t\right\}\right]. \tag{2.23}$$

If $m\ddot{x}$ is greater than the maximum value of the friction force, the load starts to slide on the trough.

For the trough, the kinetic energy is

$$T = \frac{1}{2}M\dot{Z}^2 + \frac{1}{2}m\left(\dot{Z}\sin\beta\right)^2, \tag{2.24}$$

the potential energy is

$$V = \frac{1}{2}k_1 Z^2 + \frac{1}{4}k_2 Z^4 + (mg\sin\beta)Z, \tag{2.25}$$

and the Rayleigh Dissipation Function is

$$D = \frac{1}{2}c\dot{Z}^2, \tag{2.26}$$

If Newton's second law of motion is written along the $Y$-axis (vertical) direction for the load on trough,

$$f = \mu N. \tag{2.27}$$

Here $f$ is the friction force affecting on the load and $a_y$ is vertical component of trough's acceleration:

$$\begin{gathered}\sum F_Y = ma_Y = m\ddot{Y}_t, \qquad -mg + N = m\ddot{Z}\sin\beta, \qquad N = m\left(-g + \ddot{Z}\sin\beta\right).\\ f = \mp\mu m\left(-g + \ddot{Z}\sin\beta\right),\\ Q_Z = \mp\mu m\left(\ddot{Z}\sin\beta - g\right)\cos\beta.\end{gathered} \tag{2.28}$$

If it is taken $z$ the displacement of the trough from the equilibrium position 0 (positive upward). $Mg\sin\beta = (k_1\delta_{st} + k_2\delta_{st}^3)$, where $\delta_{st}$ represents the elongation of the spring at the equilibrium position:

$$\left[M + m\left(\sin^2\beta \pm \mu\sin\beta\cos\beta\right)\right]\ddot{Z} + c\dot{Z} + k_1 Z + k_2 Z^3 = F(t) - mg\left(\sin\beta \pm \mu\cos\beta\right) \tag{2.29}$$

$$\ddot{Z} + \omega_n^2 Z = \frac{1}{\left[M + m\left(\sin^2\beta \pm \mu\sin\beta\cos\beta\right)\right]}\left[F(t) - mg\left(\sin\beta \pm \mu\cos\beta\right) - c\dot{Z} - k_2 Z^3\right] \tag{2.30}$$

Rewriting (2.29), where $\mu$ is the coefficient of friction between the materials and the trough, $\omega_n^2 = k_1/(M + m(\sin^2\beta \pm \mu\sin\beta\cos\beta))$, $\varepsilon = 1/(M + m(\sin^2\beta \pm \mu\sin\beta\cos\beta))$, $2b = c$, $\alpha = k_2$, $G = mg/(M + m(\sin^2\beta \pm \mu\sin\beta\cos\beta))$, and

$$\ddot{Z} + \omega_n^2 Z = \varepsilon\left[F\sin(\theta + \psi) - 2b\dot{Z} - \alpha Z^3\right] - G\left(\sin\beta \pm \mu\cos\beta\right). \tag{2.31}$$

## 3. Approximate Analytical Solution

The method of multiple scales is used to obtain approximate analytical solution of (2.8), (2.21), and (2.31) [13–16]. We seek a second-order expansion in the form

$$z(t,\varepsilon) \approx z_0(T_0, T_1) + \varepsilon z_1(T_0, T_1) + \ldots, \tag{3.1}$$

where the fast scale $T_0 = t$ and the slow scale $T_1 = \varepsilon t$. The time derivatives transform according to

$$\frac{d}{dt} = D_0 + \varepsilon D_1 + \ldots, \qquad \frac{d^2}{dt^2} = D_0^2 + 2\varepsilon D_0 D_1 + \ldots, \tag{3.2}$$

where $D_n = \partial/\partial T_n$. Then,

$$z' \approx D_0 z_0 + \varepsilon(D_1 z_0 + D_0 z_1), \qquad z'' \approx D_0^2 z_0 + \varepsilon\left(2D_0 D_1 z_0 + D_0^2 z_1\right). \tag{3.3}$$

Substituting (3.1)–(3.3) into (2.8) and equating coefficients of like powers $\varepsilon$, where $\Omega$ is excitation frequency, we obtain

$$\begin{aligned} D_0^2 z_0 + \omega_n^2 z_0 &= 0, \\ D_0^2 z_1 + \omega_n^2 z_1 &= -2D_0 D_1 z_0 - 2bD_0 z_0 - \alpha z_0^3 + F\sin(\Psi + T_0\Omega). \end{aligned} \tag{3.4}$$

Substituting (3.1)–(3.3) into (2.21) and equating coefficients of like powers $\varepsilon$, we obtain

$$\begin{aligned} D_0^2 z_0 + \omega_n^2 z_0 &= G\sin(\beta), \\ D_0^2 z_1 + \omega_n^2 z_1 &= -2D_0 D_1 z_0 - 2bD_0 z_0 - \alpha z_0^3 + F\sin(\Psi + T_0\Omega). \end{aligned} \tag{3.5}$$

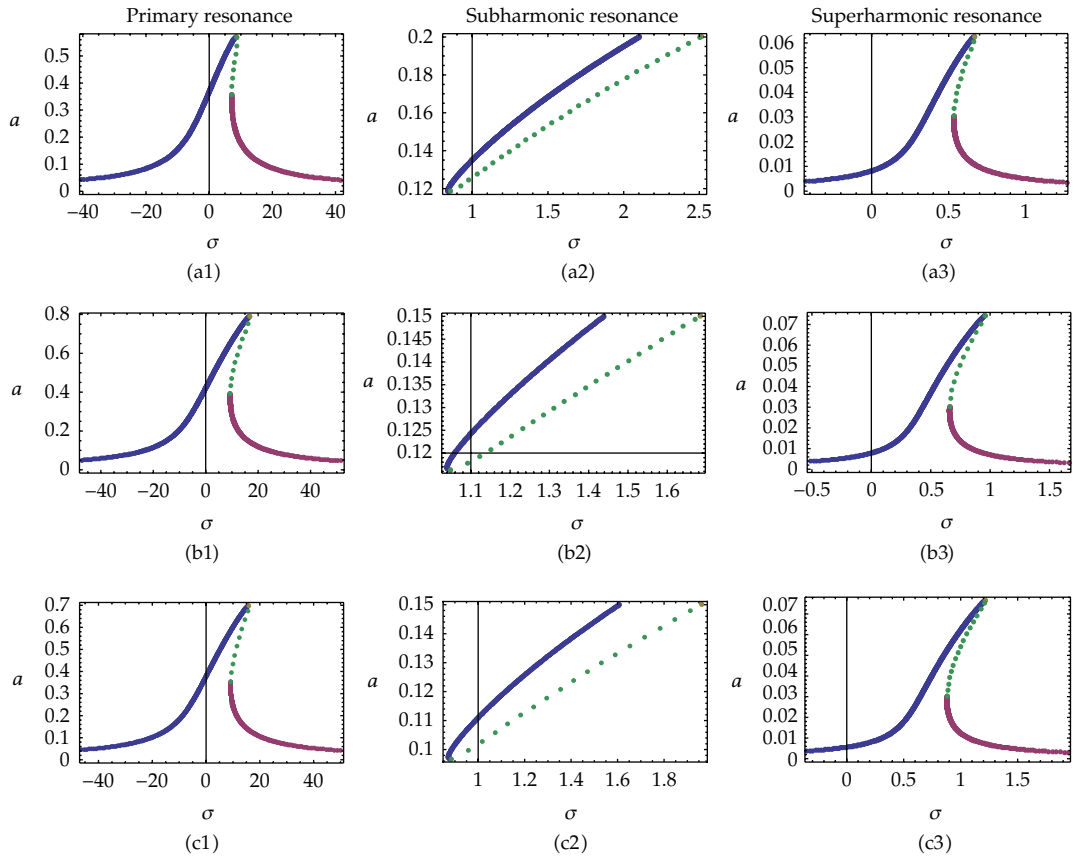


**Figure 3:** Primary resonance, subharmonic resonance and superharmonic resonance, frequency-response curve with stability, ~ stable, ⋯ unstable: (a1) conveyer empty, ($\sigma$ = 7.1179−8.72643, $a$ = 0.35701−0.57001), (b1) slide mode, ($\sigma$ = 9.41227 – 16.9651, $a$ = 0.39201 – 0.79101); (c1) ride mode, ($\sigma$ = 9.19323 – 15.9651, $a$ = 0.35401–0.69801); (a2) conveyer empty, ($\sigma$ = 0.853726 – 2.51325, $a$ = 0.1186 – 0.2001), (b2) slide mode, ($\sigma$ = 1.04791 – 1.68339, $a$ = 0.11631 – 0.15001), and (c2) ride mode, ($\sigma$ = 0.885482 – 1.96345, $a$ = 0.09681 – 0.15001). and (a3) conveyer empty, ($\sigma$ = 0.534199 – 0.667969, $a$ = 0.0305 – 0.0625), (b3) slide mode, ($\sigma$ = 0.554249 – 0.703279, $a$ = 0.0305 – 0.0636), and (c3) ride mode, ($\sigma$ = 0.880504 – 1.21958, $a$ = 0.0302 – 0.0765).

Substituting (3.1)–(3.3) into (2.31) and equating coefficients of like powers $\varepsilon$, we obtain:

$$D_0^2 z_0 + z_0 = G\mu\cos(\beta) - G\sin(\beta),$$
$$D_0^2 z_1 + \omega_n^2 z_1 = -2D_0 D_1 z_0 - 2bD_0 z_0 - \alpha z_0^3 + F\sin(\Psi + T_0\Omega). \tag{3.6}$$

This system analyzed the stability $(a,\ \gamma)$ in the equilibrium point, using (3.9), (3.12), (3.14), (3.18), (3.20), (3.22), (3.25), (3.27), and (3.29), where $J$ is Jacobian matrix of (3.10), and stability of the approximate solutions depends on the value of the eigenvalues of the Jacobian matrix $J$. The solutions are unstable if the real part of the eigenvalues is positives [13, 14]. (Figure 3) shows the frequency-response curves for primary, subharmonic, and superharmonic resonance of the vibratory conveyor. These curves show that the nonlinearity bends the frequency-response curves. The bending of the frequency-response curves leads

to multivalued amplitudes and hence to jump phenomenon. In contrast linear systems, the mass-nonlinear spring system exhibits no resonance (Figure 3).

### 3.1. Primary Resonances: $\Omega \approx \omega_0$ (Table 1)

Eliminating secular terms in equations, for analyzing the case of primary resonance, we chose the detuning parameter $\sigma$, where $a$ and $\beta$ are real,

$$\Omega = \omega_0 + \varepsilon\sigma \tag{3.7}$$

taking

$$A[T_1,\ T_2] = \frac{a[T_1]}{2} e^{i\beta[T_1]} \tag{3.8}$$

and, separating real and imaginary parts, the system of equations is solved.

(i) *Flight phase*:

$$a' = -ab - \frac{F\cos(\gamma)}{2\omega_n}$$
$$\gamma' = \frac{-3a^3\alpha + 8a\sigma\omega_n + 4F\sin(\gamma)}{8a\omega_n}, \qquad \gamma = T_1\sigma + \psi - \beta(T_1), \tag{3.9}$$

$$f_1 = a', \qquad f_2 = \gamma', \qquad f = \{\partial_a f_1,\ \partial_\gamma f_1\}, \quad \{\partial_a f_2,\ \partial_\gamma f_2\} \tag{3.10}$$

$$J = \begin{bmatrix} -b & -ab \\ \dfrac{b}{a} - \dfrac{3a\alpha}{4\omega_n} & -\sigma + \dfrac{3a^2\alpha}{8\omega_n} \end{bmatrix}. \tag{3.11}$$

(ii) *Ride phase*:

$$a' = -ab - \frac{F\cos(\gamma)}{2\omega_n}$$
$$\gamma' = \frac{-6aG^2\alpha - 3a^3\alpha\omega_n^4 + 8a\sigma\omega_n^5 + 6aG^2\alpha\cos(2\beta) + 4F\omega_n^4\sin(\gamma)}{8a\omega_n^5}, \qquad \gamma = T_1\sigma + \psi - \beta(T_1) \tag{3.12}$$

$$J = \begin{bmatrix} -b & -ab \\ \dfrac{b}{a} - \dfrac{3a\alpha}{4\omega_n} & \dfrac{6G^2\alpha + \omega_n^4(3a^2\alpha - 8\omega_n) - 6G^2\alpha\cos(2\beta)}{8\omega_n^5} \end{bmatrix}. \tag{3.13}$$

**Table 1:** Primary resonance: vibratory conveyer parameters in SI units.

| Conveyer | $\varepsilon$ | $\mu$ | $c$ | $\omega$ | $r$ | $F$ | $k_1$ | $k_2$ | $G$ | $M$ | $m$ |
|---|---|---|---|---|---|---|---|---|---|---|---|
| Empty | 0.01 | — | 6 | 14.1421 | 0.002 | 48.4 | $2\times10^4$ | 1000 | — | 100 | — |
| Ride | 0.00666667 | — | 6 | 11.547 | 0.002 | 48.4 | $2\times10^4$ | 1000 | 3.27 | 100 | 50 |
| Slide | 0.00707515 | 0.4 | 6 | 13.8782 | 0.002 | 48.4 | $2\times10^4$ | 1000 | 3.47036 | 100 | 50 |

(iii) *Slide phase*:

$$a' = -ab - \frac{F\cos(\gamma)}{2\omega_n}$$

$$\gamma' = \frac{1}{8a\omega_n^5}\left(a\left(-6G^2\alpha\left(1+\mu^2\right)+\omega_n^4\left(-3a^2\alpha+8\sigma\omega_n\right)+6G^2\alpha\left(-\left(-1+\mu^2\right)\cos(2\beta)+2\mu\sin(2\beta)\right)\right)\right.$$

$$\left.+4F\omega_n^4\sin(\gamma)\right), \qquad \gamma = T_1\sigma + \psi - \beta(T_1)$$

$$J = \begin{bmatrix} -b & -ab \\ \dfrac{b}{a} - \dfrac{3a\alpha}{4\omega_n} & \mathscr{A} \end{bmatrix}, \tag{3.14}$$

where $\mathscr{A}$ denotes $(1/8\omega_n^5)(6G^2\alpha(1+\mu^2)+\omega_n^4(3a^2\alpha-8\sigma\omega_n)+6G^2\alpha((-1+\mu^2)\cos(2\beta)-2\mu\sin(2\beta)))$.

### 3.2. Subharmonic Resonances: $\Omega \approx 3\omega_0$ (Table 2)

Eliminate secular terms in equations, for analyzing the case of subharmonic resonance, where

$$\cos(\theta_0 + \varepsilon\theta_1) = \cos(\theta_0) + O(\varepsilon), \qquad \sin(\theta_0 + \varepsilon\theta_1) = \sin(\theta_0) + O(\varepsilon),$$

$$\Lambda = \frac{-\kappa\ \Omega^2}{\left(\Omega^2 - \omega_0^2\right)} \tag{3.15}$$

near resonance

$$D_0\theta_0 = \Omega,$$

$$\Omega = 3\omega_0 + \varepsilon\sigma. \tag{3.16}$$

The solution of (3.17) can be written as

$$\theta_0 = \Omega T_0 = 3\omega_0 T_0 + \sigma T_1 \tag{3.17}$$

and, separating real and imaginary parts, the system of equations is solved.

**Table 2:** Subharmonic resonance: vibratory conveyer parameters in SI units.

| Conveyer | $\varepsilon$ | $\mu$ | $c$ | $\omega$ | $r$ | $F$ | $k_1$ | $k_2$ | $G$ | $M$ | $m$ |
|---|---|---|---|---|---|---|---|---|---|---|---|
| Empty | 0.01 | — | 0.1 | 10 | 0.02 | 1800 | $1 \times 10^4$ | 500 | — | 100 | — |
| Ride | 0.00666667 | — | 0.1 | 8.16497 | 0.02 | 1800 | $1 \times 10^4$ | 500 | 3.27 | 100 | 50 |
| Slide | 0.00707515 | 0.4 | 0.1 | 9.81337 | 0.02 | 1800 | $1 \times 10^4$ | 500 | 3.47036 | 100 | 50 |

(i) *Flight phase*:

$$a' = -\frac{a\left(8b\omega_n + 3a\alpha\Lambda\cos(\gamma)\right)}{8\omega_n}$$

$$\gamma' = \frac{-9\alpha\left(a^2 + 2\Lambda^2\right) + 8\sigma\omega_n + 9a\alpha\Lambda\sin(\gamma)}{8\omega_n}, \qquad \gamma = T_1\sigma + \psi - 3\beta(T_1),\ \Lambda = \frac{K\Omega^2}{\left(\Omega^2 - \omega_n^2\right)} \tag{3.18}$$

$$J = \begin{bmatrix} -b + \dfrac{2\sigma}{3} - \dfrac{3\alpha 8\left(a^2 + 2\Lambda^2\right)}{4\omega_n} & -ab \\ -\dfrac{3b}{a} - \dfrac{9a\alpha}{4\omega_n} & -\sigma + \dfrac{9\alpha\left(a^2 + 2\Lambda^2\right)}{8\omega_n} \end{bmatrix}. \tag{3.19}$$

(ii) *Ride phase*:

$$a' = -\frac{a\left(8b\omega_n + 3a\alpha\Lambda\cos(\gamma)\right)}{8\omega_n}$$

$$\gamma' = \frac{-18G^2\alpha - 9\alpha\left(a^2 + 2\Lambda^2\right)\omega_n^4 + 8\sigma\omega_n^5 + 18G^2\alpha\cos(2\beta) + 9a\alpha\Lambda\omega_n^4\sin(\gamma)}{8\omega_n^5}, \tag{3.20}$$

$$\gamma = T_1\sigma + \psi - 3\beta(T_1), \qquad \Lambda = \frac{K\Omega^2}{\left(\Omega^2 - \omega_n^2\right)}$$

$$J = \begin{bmatrix} \mathcal{B} & -ab \\ -\dfrac{3b}{a} - \dfrac{9a\alpha}{4\omega_n} & \mathcal{C} \end{bmatrix}, \tag{3.21}$$

where $\mathcal{B}$ denotes $-(1/12\omega_n^5)(18G^2\alpha + \omega_n^4(9a^2\alpha + 18\alpha\Lambda^2 + 12b\omega_n - 8\sigma\omega_n) - 18G^2\alpha\cos(2\beta))$ and $\mathcal{C}$ denotes $(1/8\omega_n^5)(18G^2\alpha + \omega_n^4(9\alpha(a^2 + 2\Lambda^2) - 8\sigma\omega_n) - 18G^2\alpha\cos(2\beta))$.

(iii) *Slide phase*:

$$a' = -0.05a - 0.429898a^2\cos(\gamma)$$
$$\gamma' = 1.37347 \times 10^{-6}\left(-155304. + 9274.12\left(-4500\left(0.0010125 + a^2\right) + 78.507\sigma\right)\right. \tag{3.22}$$
$$\left. +939005.a\sin(\gamma)\right), \qquad \gamma = T_1\sigma + \psi - 3\beta(T_1),$$

$$J = \begin{bmatrix} \mathfrak{D} & -0.05a \\ -\dfrac{0.15}{a} - 114.64a & \mathcal{E} \end{bmatrix}, \tag{3.23}$$

where $\mathfrak{D}$ denotes $-9.15646 \times 10^{-7}(155304. + 4.217335 \times 10^7(0.0010125 + a^2) + 364042.(0.15 - 2\sigma))$ and $\mathcal{E}$ denotes $1.37347 \times 10^{-6}(155304. + 9274.12(4500(0.0010125 + a^2) - 78.507\sigma))$.

### *3.3. Superharmonic Resonances:* $\Omega \approx 1/3\omega_0$ *(Table 3)*

Eliminating secular terms in equations, for analyzing the case of superharmonic resonance, where

$$3\Omega = \omega_0 + \varepsilon\sigma$$
$$3\Omega T_0 = (\omega_0 + \varepsilon\sigma)T_0 = \omega_0 T_0 + \sigma\varepsilon T_0 = \omega_0 T_0 + \sigma T_1 \tag{3.24}$$

and, separating real and imaginary parts, the system of equations is solved.

(i) *Flight phase*:

$$a' = -ab + \frac{\alpha\Lambda^3\cos(\gamma)}{8\omega_n}$$
$$\gamma' = -\frac{3a^3\alpha + 6a\alpha\Lambda^2 - 8a\sigma\omega_n + \alpha\Lambda^3\sin(\gamma)}{8a\omega_n}, \qquad \gamma = T_1\sigma + 3\psi - \beta(T_1) \tag{3.25}$$

$$J = \begin{bmatrix} -b & -ab \\ \dfrac{b}{a} - \dfrac{3a\alpha}{4\omega_n} & -\sigma + \dfrac{3\alpha\left(a^2 + 2\Lambda^2\right)}{8\omega_n} \end{bmatrix}. \tag{3.26}$$

**Table 3:** Superharmonic resonance: vibratory conveyer parameters in SI units.

| Conveyer | $\varepsilon$ | $\mu$ | $c$ | $\omega$ | $r$ | $F$ | $k_1$ | $k_2$ | $G$ | $M$ | $m$ |
|---|---|---|---|---|---|---|---|---|---|---|---|
| Empty | 0.01 | — | 0.1 | 10 | 0.4 | 444.444 | $1 \times 10^4$ | 2000 | | 100 | — |
| Ride | 0.00666667 | — | 0.1 | 8.16497 | 0.4 | 444.444 | $1 \times 10^4$ | 2000 | 3.27 | 100 | 50 |
| Slide | 0.00707515 | 0.4 | 0.1 | 9.81337 | 0.4 | 444.444 | $1 \times 10^4$ | 2000 | 3.47036 | 100 | 50 |

(ii) *Ride phase*:

$$a' = -ab + \frac{\alpha\Lambda^3 \cos(\gamma)}{8\omega_n}$$

$$\gamma' = \frac{a\left(-6G^2\alpha - 3\alpha\left(a^2 + 2\Lambda^2\right)\omega_n^4 + 8\sigma\omega_n^5\right) + 6aG^2\alpha\cos(2\beta) - \alpha\Lambda^3\omega_n^4\sin(\gamma)}{8a\omega_n^5}, \tag{3.27}$$

$$\gamma = T_1\sigma + 3\psi - \beta(T_1)$$

$$J = \begin{bmatrix} -b & -ab \\ \dfrac{b}{a} - \dfrac{3a\alpha}{4\omega_n} & \dfrac{6G^2\alpha + \omega_n^4\left(3a^2\alpha + 6\alpha\Lambda^2 - 8\sigma\omega_n\right) - 6G^2\alpha\cos(2\beta)}{8\omega_n^5} \end{bmatrix}. \tag{3.28}$$

(iii) *Slide phase*:

$$a' = -ab - \frac{\alpha\Lambda^3 \cos(\gamma)}{8\omega_n}$$

$$\begin{aligned} \gamma' = \frac{1}{8a\omega_n^5}\Big(a\Big(-6G^2\alpha\left(1+\mu^2\right) + \omega_n^4\Big(-3\alpha\left(a^2+2\Lambda^2\right) + 8\sigma\omega_n\Big) \\ +6G^2\alpha\Big(-\left(-1+\mu^2\right)\cos(2\beta) + 2\mu\sin(2\beta)\Big)\Big) + \alpha\Lambda^3\omega_n^4\sin(\gamma)\Big) \end{aligned} \tag{3.29}$$

$$\gamma = T_1\sigma + \psi - \beta(T_1)$$

$$J = \begin{bmatrix} -b & -ab \\ \dfrac{b}{a} - \dfrac{3a\alpha}{4\omega_n} & \mathcal{F} \end{bmatrix}, \tag{3.30}$$

where $\mathcal{F}$ denotes $(1/8\omega_n^5)(6G^2\alpha(1+\mu^2) + \omega_n^4(3a^2\alpha + 6\alpha\Lambda^2 - 8\sigma\omega_n) + 6G^2\alpha((-1+\mu^2)\cos(2\beta) - 2\mu\sin(2\beta)))$.

## 4. Numerical Results

The numerical calculations of the vibrating system are performed with the help of the software Mathematica [17, 18]. Figures 4, 5, and 6 show the displacement-time response, the power spectrum, phase portrait, and Poincaré map for the primary, subharmonic, and superharmonic resonance. By Poincaré map I concludes that the motion of the oscillator is periodic with period-1.

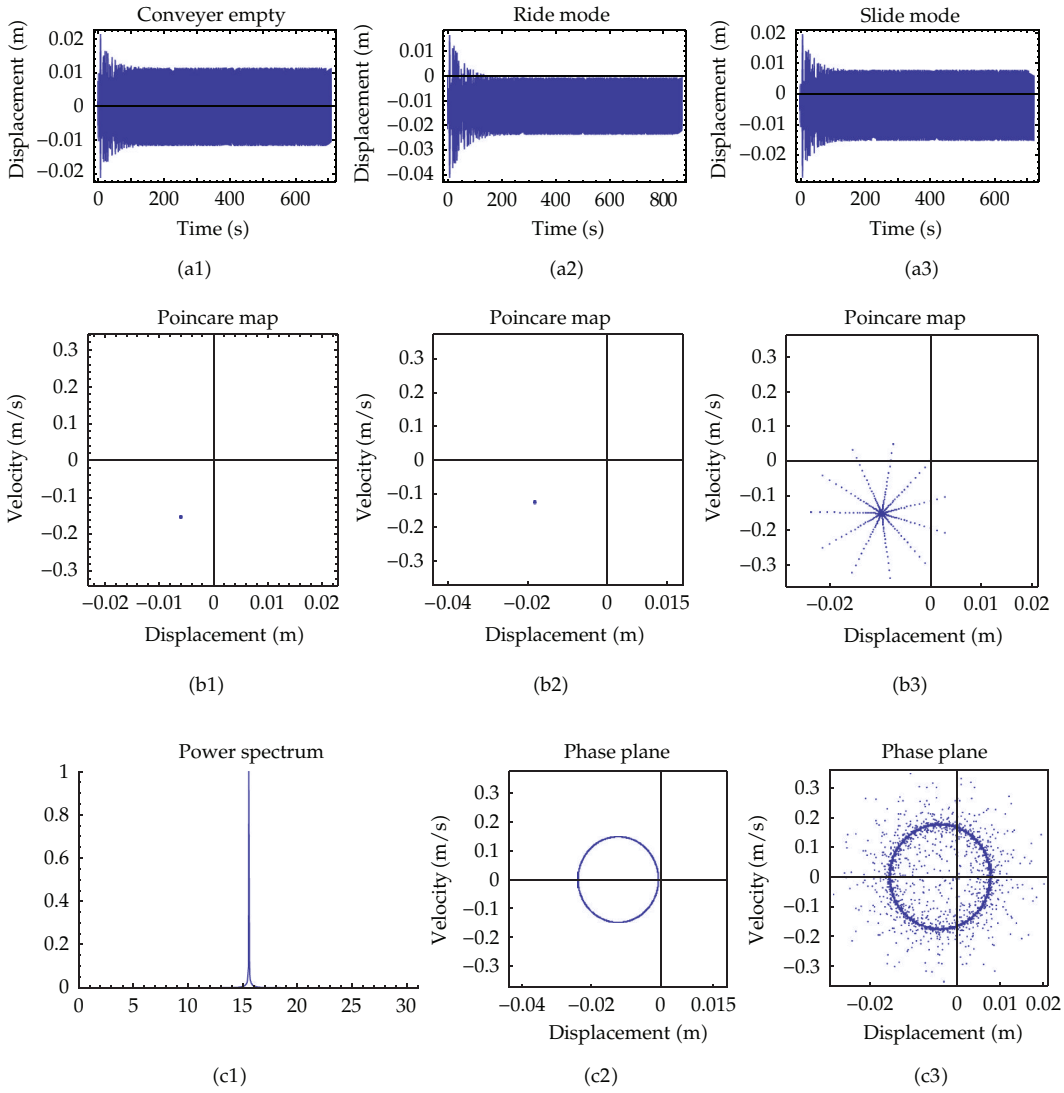


**Figure 4:** Primary resonance: (a) displacement-time response, (b3) Poincaré map (before stabilization), fixed points (stable focus), (b1), (b2) Poincaré map (after stabilization), (c1) power spectrum, (c2) phase portrait (after stabilization), (c3) phase portrait (before stabilization).

In Figures 4, 5, and 6, the curves obtained numerically and analytically by solving (2.8), (2.21), and (2.31) are plotted. The main characteristic values used in this study are given in Tables 1, 2, and 3.

## 5. Conclusions

In this study, the transition over resonance of a nonlinear vibratory system, excited by crank-and-rod, is important in terms of the maximum vibrational amplitude produced on the drive for the crossover. The maximum amplitude of vibration is then of interest

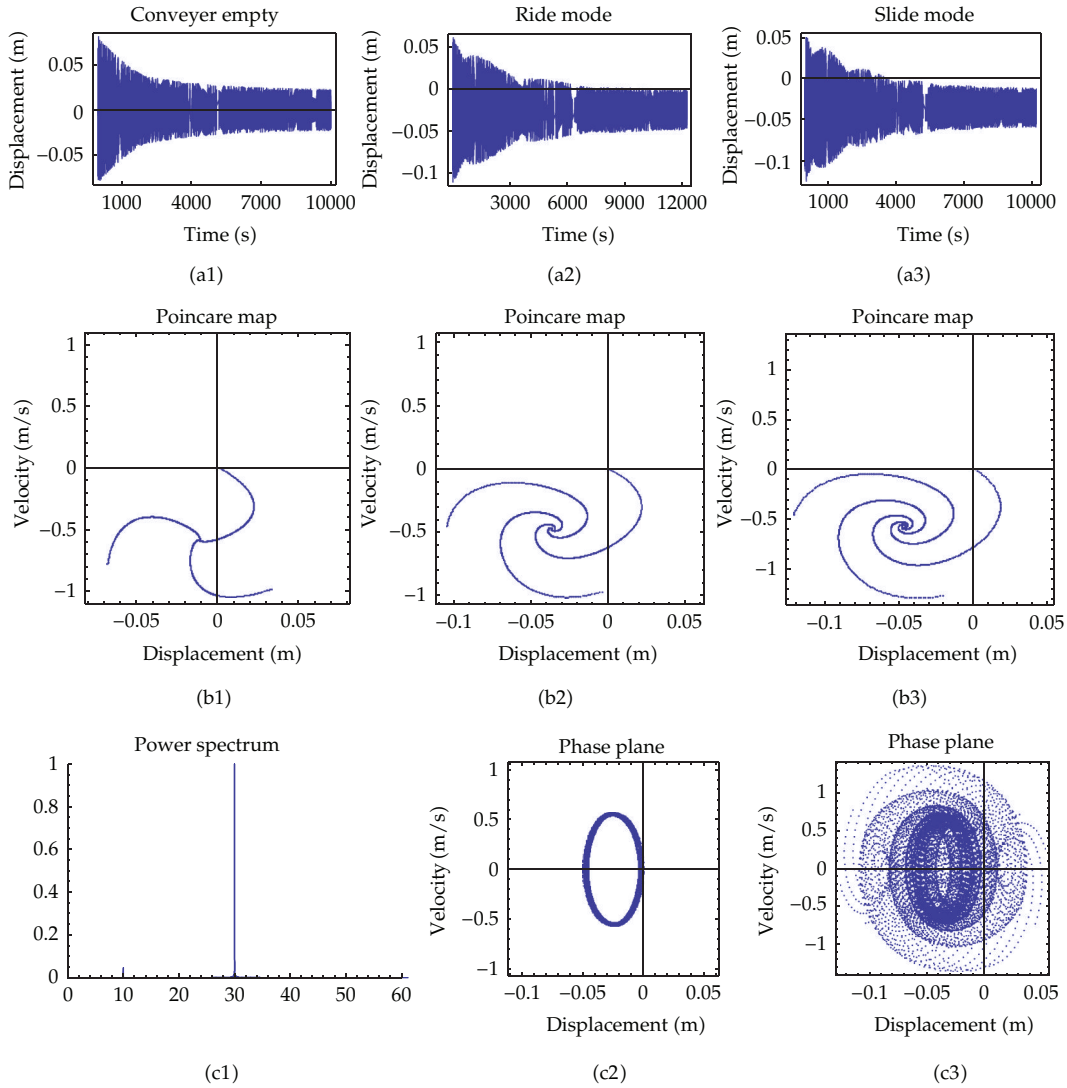


**Figure 5:** Subharmonic resonance: (a) displacement-time response, (b3) Poincaré map (before stabilization), fixed points (stable focus), (b1), (b2) Poincaré map (after stabilization), (c1) power spectrum, (c2) phase portrait (after stabilization), (c3) phase portrait (before stabilization).

in determining the structural safety of the vibrating members. The shaded region in the amplitude-frequency plot is unstable; the extend of unstableness depends on a number of factors such as the amount of damping present, nonlinearity of spring, and the rate of chance of the exciting frequency (Figure 3). Results of the numerical simulations, obtained from the analytical equations, showed that the important dynamic characteristics of the system, such as damping, nonlinearity and the amplitude excitations effects, still presented a periodic behavior for these situations. The bending of the response is due to the nonlinearity, and is responsible for a jump phenomenon. In the motion of the system near resonance the jump phenomenon occurs. A periodic solution in the case of the angular velocity taken above the resonance (after stabilization) is illustrated in Figure 4.

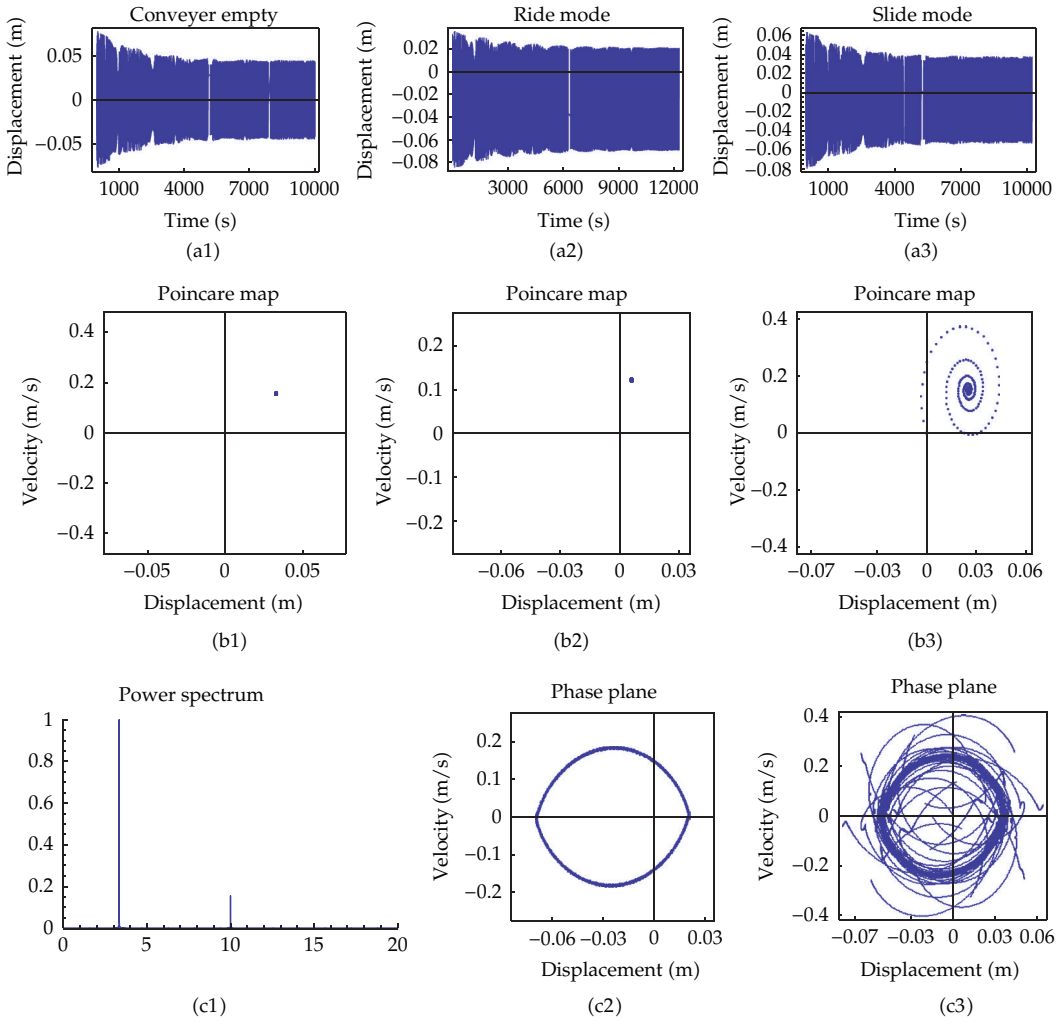


**Figure 6:** Superharmonic resonance: (a) displacement-time response, (b3) Poincaré map (before stabilization), fixed points (stable focus), (b1), (b2) Poincaré map (after stabilization), (c1) power spectrum, (c2) phase portrait (after stabilization), (c3) phase portrait (before stabilization).

Comparing the results obtained by applying the approximate analytic method with those obtained numerically it is concluded that the difference is negligible, proving the correctness of the analytic procedure used.

In the future, it is possible to investigate this system with the nonideal source, and nonideal vibrating systems are those for which the power supply is limited. Nonideal problems are more realistic, and the model should take into account also the influence of the dynamics of the oscillating mechanical elements on electrical properties of the DC motor [5].

## Acknowledgment

The author greatly appreciates the comments of an anonymous referee.

## References


[1] V. O. Konokenko, *Vibrating Problems With a Limited Power Supply*, Ilife, London, UK, 1969.

[2] D. Belato, H. I. Weber, J. M. Balthazar, and D. T. Mook, "Chaotic vibrations of a nonideal electro-mechanical system," *International Journal of Solids and Structures*, vol. 38, no. 10–13, pp. 1699–1706, 2001.

[3] D. Belato, J. M. Balthazar, and H. I. Weber, "A note about the appearance of non-hyperbolic solutions in a mechanical pendulum system," *Nonlinear Dynamics*, vol. 34, no. 3-4, pp. 309–317, 2003.

[4] J. M. Balthazar, D. T. Mook, H. I. Weber et al., "An overview on non-ideal vibrations," *Meccanica*, vol. 38, no. 6, pp. 613–621, 2003.

[5] J. M. Balthazar, R. M. L. R. F. Brasıl, H. I. Weber et al., "A review of new vibration issues due to non-ideal energy sources," in *Dynamical Systems and Control*, CRC Press, LLC, Boca Raton, Fla, USA, 2004.

[6] G. F. Alışverişçi, "Computational dynamic analysis of vibrational conveyers with single-mass; crank-and-rod exciters," in *Proceedings of the 6th International Conference of the Balkan Physical Union Book Series: AIP Conference Proceedings*, vol. 899, pp. 373–374, August 2007.

[7] S. Ganapathy and M. A. Parameswaran, "Effect of material loading on the starting and transition over resonance of a vibratory conveyor," *Mechanism and Machine Theory*, vol. 22, no. 2, pp. 169–176, 1987.

[8] M. R. Bolla, J. M. Balthazar, J. L. P. Felix, and D. T. Mook, "On an approximate analytical solution to a nonlinear vibrating problem, excited by a nonideal motor," *Nonlinear Dynamics*, vol. 50, no. 4, pp. 841–847, 2007.

[9] A. O. Spivakovasky and V. K. Dyachkov, *Conveying Machines, Volume (I, II)*, Mir Publichers, Moscow, Russia, 1985.

[10] A. Götzendorfer, *Vibrated Granular Matter: Transport, Fluidization, and Patterns*, PhD University Bayreuth, Bavaria, Germany, 2007.

[11] M. A. Parameswaran and S. Ganapathy, "Vibratory conveying-analysis and design: a review," *Mechanism and Machine Theory*, vol. 14, no. 2, pp. 89–97, 1979.

[12] I. I. Blekhman, G. Yu, and D. G. Ju, *Vibrational Displacement*, Nauka, Moscow, Russia, 1964.

[13] A. H. Nayfeh and D. T. Mook, *Nonlinear Oscillations*, Wiley-Interscience, New York, NY, USA, 1979.

[14] G. Schmidt and A. Tondl, *Nonlinear Vibrations*, Cambridge University Press, Cambridge, UK, 1986.

[15] A. H. Nayfeh and B. Balachandran, *Applied Nonlinear Dynamics: Analitical, Computation and Experimental Methods*, John Wiley & Sons, New York, NY, USA, 1995.

[16] A. H. Nayfeh, "Resolving controversies in the application of the method of multiple scales and the generalized method of averaging," *Nonlinear Dynamics. An International Journal of Nonlinear Dynamics and Chaos in Engineering Systems*, vol. 40, no. 1, pp. 61–102, 2005.

[17] A. H. Nayfeh and C. M. Chin, *Methods with Mathematica*, 1999.

[18] S. Lynch, *Dynamical Systems with Applications using Mathematica*, Birkhäuser Boston, Boston, MA, usa, 2007.